

# Reliability Optimization of Friction-Damped Systems Using Nonlinear Modes

Malte Krack<sup>1,\*</sup>, Sebastian Tatzko<sup>1</sup>, Lars Panning-von Scheidt<sup>1</sup>, Jörg Wallaschek<sup>1</sup>

---

## Abstract

*A novel probabilistic approach for the design of mechanical structures with friction interfaces is proposed. The objective function is defined as the probability that a specified performance measure of the forced vibration response is achieved subject to parameter uncertainties. The practicability of the approach regarding the extensive amount of required design evaluations is strictly related to the computational efficiency of the nonlinear dynamic analysis. Therefore, it is proposed to employ a recently developed parametric reduced order model (ROM) based on nonlinear modes of vibration, which can facilitate a decrease of the computational burden by several orders of magnitude.*

*The approach was applied to a rotationally periodic assembly of a bladed disk with underplatform friction dampers. The robustness of the optimum damper design was significantly improved compared to the deterministic approach, taking into account uncertainties in the friction coefficient, the excitation level and the linear damping. Moreover, a scale invariance for piecewise linear contact constraints is proven, which can be very useful for the reduction of the numerical effort for the analysis of such systems.*

**Keywords:** nonlinear modes, friction damping, underplatform dampers, turbomachinery bladed disks, robust design, reliability, uncertainties, scale invariance

---



---

\*Corresponding author

Email address: [krack@ila.uni-stuttgart.de](mailto:krack@ila.uni-stuttgart.de) (Malte Krack)

## Nomenclature

$EO$	Engine order
$f$	Probability density function
$\mathbf{f}_e$	Excitation force vector
$\mathbf{g}$	Nonlinear force vector
$H$	Heaviside function
$k_n, k_t$	Normal and tangential contact stiffness
$m, m_{\text{opt},c}$	Friction damper mass, optimum mass without uncertainties
$\mathbf{M}, \mathbf{C}, \mathbf{K}$	Mass, damping, stiffness matrix
$N_h$	Harmonic order of Fourier ansatz
$p_0, p_n, \mathbf{p}_t$	Initial normal pressure, normal and tangential contact pressure
$\text{Pr}$	Probability
$q$	Modal amplitude defined as kinetic energy
$t$	Time
$\mathbf{u}$	Displacement vector
$X, X_{\text{DV}}, X_{\text{UC}}$	System parameter, design variable, uncertain parameter
$\varepsilon$	Excitation level
$\eta$	Hysteretic damping ratio
$\lambda, \omega_0, D$	Eigenvalue, eigenfrequency, damping ratio
$\mu$	Friction coefficient
$\Omega, \Omega_r$	Excitation frequency, rotational speed

$\Theta$	Performance measure
$(\dot{\phantom{x}}), (\ddot{\phantom{x}})$	First and second-order time derivative
$(\phantom{x})^T$	Transpose
DOF	Degree of freedom
FE	Finite Element
FRF	Frequency response function
HBM	(High-order) Harmonic Balance Method
NMA	Nonlinear Modal Analysis
ODE	Ordinary Differential Equation
ROM	Reduced Order Model

## 1. Introduction

*Friction damping.* Friction damping represents an established technology for the passive reduction of forced vibrations. Various industrial applications exist in the field of turbomachinery, where friction joints are introduced in order to improve the dynamical behavior and increase the mechanical integrity of bladed disks [1, 2, 3, 4, 5]. Typically, the goal is to decrease the risk of fatigue by either providing enough damping in critical operating conditions or shifting eigenfrequencies away from possible coincidences with the load spectrum. The design of such friction joints is hampered by the strongly nonlinear character of the contact constraints, the large amount of structural degrees of freedom (DOF) required for the description of the vibration behavior, and the uncertain character of system parameters.

*Robust design under uncertainties.* Uncertainty can be defined as the error between the according mathematical model and reality [6]. For friction-damped mechanical structures, this deviation can occur in material and geometric properties owing to manufacturing tolerances and material imperfections. The parameters associated with the description of the contact dynamics are often dif-

difficult to determine and introduce uncertainty to the system. Similarly, the dynamic effects caused by the interaction of the underlying mechanical structure with the surrounding medium can often not be modeled accurately. Particularly, spatial and spectral distributions of excitation forces are typical examples for uncertain system parameters.

It appears to be common practice in the field of friction damping to tune the design for only a single set of nominal parameters, i.e. to perform a so-called Single-Point-Optimization, regardless of the parameter uncertainties [7, 8, 9]. If the variability of uncertain parameters is not properly taken into account in the design process, even high-fidelity models cannot yield optimum designs with respect to robustness. Hence, this localized optimization can result in a design that is highly sensitive to even slight changes in the parameters [10].

Several authors addressed uncertainty in terms of non-probabilistic, post-optimality sensitivity analysis. Cameron et al. [11] introduced the terminology of the damper performance curve and employed this strategy to find a design point that is widely reliable with respect to variations in the excitation level and the linear damping. Cha and Sinha [12] numerically determined the optimum normal preload of a friction damper that is largely insensitive regarding different types of excitation. Several approaches are known for the analysis of the stochastic characteristics of the nonlinear forced response for stochastically distributed parameters [13, 14, 15], but they have not been applied to reliability-based design so far.

*Reduced order modeling.* Probabilistic approaches typically involve integrals over the relevant parameter domain. The evaluation of these integrals cannot be performed analytically in closed form in most cases and, thus, has to be performed numerically. This task often involves evaluations of the design performance for a large number of parameter points. This can be computationally expensive owing to the nonlinear character and considering large problem dimensions for the dynamic analysis. The practicability of probabilistic approaches for friction-damped structures therefore relies on the efficiency of the

dynamic analysis. It is thus essential to employ reduced order modeling (ROM) strategies in order to decrease the otherwise prohibitive computational costs. State-of-the-art strategies to reduce the computational effort for the dynamic analysis in this field include component mode synthesis [16], (multi-)harmonic balance [17] and direct tracing of resonances [18]. However, there still remains a demand for a more drastic order reduction in conjunction with probabilistic design approaches.

The concept of nonlinear modes can generally be employed to extract the essential signature of oscillatory nonlinear systems [19, 20] and therefore gives rise to order reduction opportunities for nonlinear systems [21, 22]. In Krack et al. [23, 24], an approach was proposed that reduces the computational effort by several orders of magnitude within reasonable ranges of validity. However, it cannot directly be employed in a sophisticated design process since the ROM lacks of an appropriate parameter space.

*Proposed approach and outline.* The objective of this study is twofold: Firstly, a novel reliability optimization strategy for the design of friction-damped mechanical structures under uncertainties is proposed. Secondly, the application of an extremely efficient parametric ROM based on nonlinear modes in course of sophisticated probabilistic design approaches is proposed.

This paper shall be regarded as a proof-of-concept study for the proposed overall design approach. Hence, only a comparatively low number of uncertain parameters was considered in the numerical example. Furthermore, the methodology was only applied to systems driven by purely harmonic forcing in vicinity of a single resonance. While this is often a reasonable assumption, it is also in accordance with the current limitations of the employed ROM which can currently treat neither generic excitation frequency spectra nor nonlinear modal interactions. An important goal of this article is to apply the design approach to an example of realistic complexity in terms of structural and contact dynamics of the intended industrial applications.

This paper is organized as follows: The description of the structural dynamic

behavior is briefly addressed in Section 2 with an emphasis on the formulation of the contact constraints and the novel scale invariance exploited for the parameter studies. The reliability optimization approach is detailed in Section 3. The nonlinear modal reduced order model is presented in Section 4 with a focus on the parameter space extended in this work. An overview of the overall proposed approach is provided in Section 5. Finally, the methodology is applied to a bladed disk with underplatform friction dampers in Section 6.

## 2. Modeling

### 2.1. Dynamic description of structures with contact interfaces

The dynamics of a spatially discrete, mechanical system is governed by a system of second-order ordinary differential equations,

$$\mathbf{M}\ddot{\mathbf{u}}(t) + \mathbf{C}\dot{\mathbf{u}}(t) + \mathbf{K}\mathbf{u}(t) + \mathbf{g}(\mathbf{u}(t), \dot{\mathbf{u}}(t)) = \mathbf{f}_e(t). \quad (1)$$

Herein,  $\mathbf{M} = \mathbf{M}^T$  is the symmetric positive definite mass matrix.  $\mathbf{C}$  and  $\mathbf{K}$  are the damping and the stiffness matrix, respectively.  $\mathbf{g}(\mathbf{u}(t), \dot{\mathbf{u}}(t))$ , and  $\mathbf{f}_e(t)$  are vectors of nonlinear and excitation forces.  $\mathbf{u}$  is the vector of generalized coordinates.

Temperature and wear effects may generally alter the material properties and the geometry of friction-damped systems. These effects typically occur on timescales that are much longer than the one associated with the vibration behavior. It is thus reasonable to consider the structural matrices and nonlinear forces in Eq. (1) as time-invariant. As generalized coordinates are allowed in Eq. (1), it is possible to apply component mode synthesis in order to reduce the dynamics of the system to the most relevant linear modes. This can be useful when dealing with large-scale structures with only localized contact joints. In this study, only the nonlinear forces associated with the contact constraints are treated as nonlinear, while all other possible sources of nonlinearity such as large deformations or nonlinear fluid-structure-interaction are not taken into account in the dynamic analysis.

## 2.2. Contact modeling

Unilateral contact in normal direction and dry Coulomb friction in the tangential plane are considered in this study. In the field of friction damping, it is common to apply elastic formulations of these contact laws and to interpret the associated elastic properties physically as contact stiffness [25, 26, 27, 28, 29]. Mathematically, the resulting constitutive laws are equivalent to penalty reformulations of the complementarity conditions with constant normal and tangential stiffness parameters  $k_n$  and  $k_t$  [30],

$$p_n(t) = (k_n u_n(t) + p_0)_+ \quad (2)$$

$$\mathbf{p}_t(t) = \begin{cases} \mathbf{0} & \text{lift-off} \\ k_t (\mathbf{u}_t(t) - \mathbf{u}_t(t_{\text{stick}})) + \mathbf{p}_t(t_{\text{stick}}) & \text{stick} \\ \mu p_n(t) \frac{\dot{\mathbf{u}}_t(t)}{\|\dot{\mathbf{u}}_t(t)\|} & \text{slip} \end{cases} \quad (3)$$

Herein,  $t_{\text{stick}}$  is the time instant at which the current stick phase began and  $\mathbf{u}_t(t_{\text{stick}}), \mathbf{p}_t(t_{\text{stick}})$  are the values just before the current stick phase began. The contact model is formulated in terms of the contact surface normal and tangential pressures  $p_n, \mathbf{p}_t$ , respectively. The friction coefficient  $\mu$  is assumed to be constant and identical for stick and slip state. The initial normal pressure  $p_0$  can be negative to account for initial clearances, see e. g. [27] for details. The contact model in Eqs. (2) and (3) separately models stick, slip and lift-off states and accounts for the effect of the normal dynamics on the friction behavior. The contact pressures have been integrated over the contact interfaces in order to obtain the vector of nonlinear forces  $\mathbf{g}$  in Eq. (1). Therefore, a node-to-node formulation was used with the matching nodes of the surface elements as integration points. Linear surface elements have been used in the case study, such that the surface integral was approximated by a weighted sum over the integration points, where the weights represent the area associated with each integration point [30]. Small relative deflections were assumed for this procedure such that nonlinearity stems solely from the contact laws, but not from the kinematics or the pressure integration scheme.

A scale invariance is exploited in this study to determine the amplitude-dependent nonlinear modes for different scaling values  $\kappa$  of the initial pressure distribution  $\kappa p_0$  from the nonlinear modes computed for a single value  $p_0$ . This scale invariance can be stated as follows:

scale invariance:

$$\begin{aligned} &\text{If } [\mathbf{u} \ \dot{\mathbf{u}}](t) \text{ is a solution to Eq. (1) for } \{[\mathbf{u} \ \dot{\mathbf{u}}]_{(t=0)}, p_0, \mathbf{f}_e(t)\}, \\ &\text{then } \kappa [\mathbf{u} \ \dot{\mathbf{u}}](t) \text{ is a solution to Eq. (1) for } \{\kappa [\mathbf{u} \ \dot{\mathbf{u}}]_{(t=0)}, \kappa p_0, \kappa \mathbf{f}_e(t)\}. \end{aligned} \quad (4)$$

Starting from a specific solution  $[\mathbf{u} \ \dot{\mathbf{u}}](t)$  corresponding to initial value  $[\mathbf{u} \ \dot{\mathbf{u}}]_{(t=0)}$ , preload  $p_0$  and loading  $\mathbf{f}_e(t)$ , this scale invariance allows to determine the solution to a scaled problem without the need for re-computation. A similar scale invariance was reported for the special case of constant normal loading in [31]. It was postulated in [23] for the more general case of variable normal contact force including lift-off. A formal proof can be found in Appendix A valid for the contact formulation applied in this paper.

The exploitation of the scale invariance can significantly increase the computational efficiency of the design process. This feature also provides a better understanding of the often reported analogy between the increase of the excitation and the decrease of the normal preload [32]. It is therefore believed that this scale invariance can be applied for a better understanding and computational effort reduction in nonlinear dynamic analyses of friction-damped structures far beyond the application to nonlinear modes.

It should be noticed that the preload scaling  $\kappa$  can not always be considered as a directly accessible parameter. In case of friction-damped rotating bladed disks, the preload is typically influenced by the pretwist design in case of shroud interfaces [33] and adjustment of damper density and geometry in case of underplatform dampers [2]. The actual preload also depends on the rotational speed and the mass and stiffness distributions of the resulting assembly.

Finally, it should be emphasized that contact laws such as piecewise nonlinear [32] or Lagrangian [34] formulations could be easily applied to the proposed methodology. However, the scale invariance will then no longer be valid in gen-



eral. Hence, the dimension of the parameter domain for which the dynamic analyses have actually to be carried out, would increase by one.

### 3. Robust design optimization

The appropriate formulation of the optimization problem for a system with uncertainties is not a trivial task. Considering the performance sensitivity in addition to the performance  $\Theta$  at the design point generally yields a multi-objective optimization problem. The solution of such problems is typically much more computationally expensive compared to single-objective problems and leads to a whole set of Pareto-optimal designs rather than a single optimum design. Instead of formulating a multi-objective problem, the robustness can also be incorporated into a single-objective criterion employing the Von-Neumann-Morgenstern statistical decision theory [10]. The optimization problem is then defined as the maximization of the expected value of the reliability, i. e. the ‘probability of success’  $\Pr [\Theta (\mathbf{X}) \geq \Theta_{\text{ref}}]$  that a specified performance  $\Theta_{\text{ref}}$  is achieved [10, 35, 36],

$$\begin{aligned} & \text{maximize} && \Pr [\Theta (\mathbf{X}) \geq \Theta_{\text{ref}}] \\ & \text{with respect to} && \mathbf{X}_{\text{DV}} \\ & \text{subject to uncertainties in} && \mathbf{X}_{\text{UC}} . \end{aligned} \quad (5)$$

The entire set of system parameters  $\mathbf{X}$  comprises the set of design variables  $\mathbf{X}_{\text{DV}}$  as well as the uncertain parameters  $\mathbf{X}_{\text{UC}}$ . Design variables may also be treated as uncertain. Thus, the system parameters are the union of design and uncertain parameters,

$$\mathbf{X} = \mathbf{X}_{\text{UC}} \cup \mathbf{X}_{\text{DV}} . \quad (6)$$

The probability of success in Eq. (5) can be expressed as expectation integral over the entire domain of all  $N_{\text{UC}}$  uncertain parameters,

$$\begin{aligned} & \Pr [\Theta (\mathbf{X}) \geq \Theta_{\text{ref}}] = \\ & \int_{X_{N_{\text{UC}},\text{min}}}^{X_{N_{\text{UC}},\text{max}}} \cdots \int_{X_{1,\text{min}}}^{X_{1,\text{max}}} H [\Theta (\mathbf{X}) - \Theta_{\text{ref}}] f_1(X_1) dX_1 \cdots f_{N_{\text{UC}}}(X_{N_{\text{UC}}}) dX_{N_{\text{UC}}} . \end{aligned} \quad (7)$$

Herein,  $H$  is the heaviside function,  $f_i$  are the probability density functions of the uncertain parameters  $X_i \in \mathbf{X}_{UC}$ .

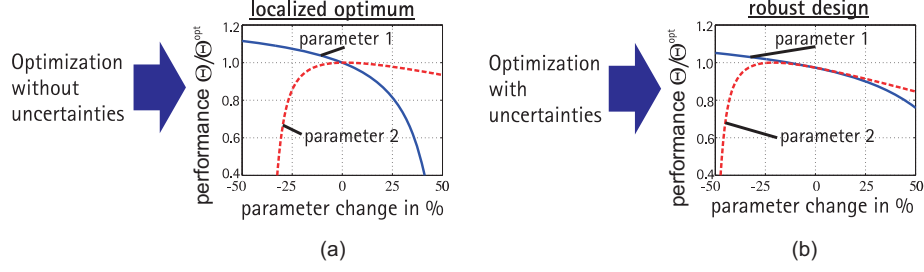


Figure 1: Qualitative comparison between localized optimization and robust design ( (a) localized optimization, (b) robust design )

Owing to the integral formulation of Eq. (7), this approach explicitly accounts for off-design performance. The optimum design will therefore deviate from the localized optimum obtained by simply maximizing performance for nominal parameters. Typically, the performance of the robust design is slightly worse for nominal parameters but exhibits a greater robustness against considerable parameter changes, see Fig. 1. Eq. (7) represents the limit case of a weighted-sum reformulation of a multi-objective problem with the qualities at every design point as the objectives and the corresponding probability values as weighting factors.

An appropriate performance measure  $\Theta$  needs to be selected for the design process. For the sought application to friction damping, conceivable measures are displacement amplitudes, dynamic stresses, strength ratios, resonance frequency or combinations of these measures. The performance threshold  $\Theta_{ref}$  could be derived from strength or fatigue analyses.

The evaluation of the probability integral can be performed analytically in some cases. In particular, if it is valid to approximate the performance  $\Theta(\mathbf{X})$  in terms of a linearized function in the parameters  $\mathbf{X}$ , analytical expressions for the reliability can be easily obtained [35]. In general, however, the integration needs to be carried out using numerical integration methods. The adaptive recursive Simpson's integration rule was employed in this study [37]. This is a conven-

tional integration method available in most engineering software frameworks. For this method, the computational cost increases exponentially with  $N_{UC}$ . In this paper, at most three uncertain variables had to be taken into account simultaneously, which still led to acceptable computational effort. When more uncertain parameters are taken into account, this integration method can soon become prohibitive. In this case, Monte-Carlo or sparse grid methods typically perform better [38]. However, those methods are more complex and feature additional parameters that need to be specified with care. Hence, those methods have not been further considered within this paper.

#### 4. Nonlinear modal reduced order model

The reliability optimization proposed in this paper could be prohibitive even for the most efficient quadrature scheme to evaluate Eq. (7), if the cost for the performance evaluation  $\Theta(\mathbf{X})$  for a single parameter point is too large. In order to avoid this, the ROM developed in [23] is used in this paper, which is based on the concept of nonlinear modes. The benefit of this ROM is that it is extremely cheap to evaluate since it leads to a scalar nonlinear algebraic equation for each parameter point. The downside is that the validity is restricted to those dynamic regimes, where the vibration energy is mainly confined to a single nonlinear mode.

In order to employ the ROM in the reliability design process, the generally parameter-dependent nonlinear modes have to be available in the whole parameter domain  $\mathbf{X}_{\min} \leq \mathbf{X} \leq \mathbf{X}_{\max}$ , see Eq. (7). For a group of parameters, a costly re-computation of the nonlinear modes can be avoided. This applies in an exact manner to the normal preload due to the scale invariance, see Subsection 2.2. This also applies approximately to parameters associated to near-resonant harmonic forcing and weak linear damping. The re-computation of the nonlinear modes is avoided by assuming that the influence of these terms on the geometry of the invariant manifold can be neglected and the modal properties can be approximated by the nonlinear modes computed for a surrogate system without

these terms [23].

It should be stressed that preload, damping and forcing parameters are often regarded as uncertain and/or relevant design variables in the field of friction damping [39, 14, 24]. Hence, the proposed parameter treatment strategy can greatly enhance the computational benefit of the nonlinear modal ROM in the course of reliability optimization of friction-damped structures. For the remaining group of parameters such as contact parameters, material properties, geometric properties or temperature, the nonlinear modes generally have to be re-computed.

## 5. Overview of the proposed reliability analysis

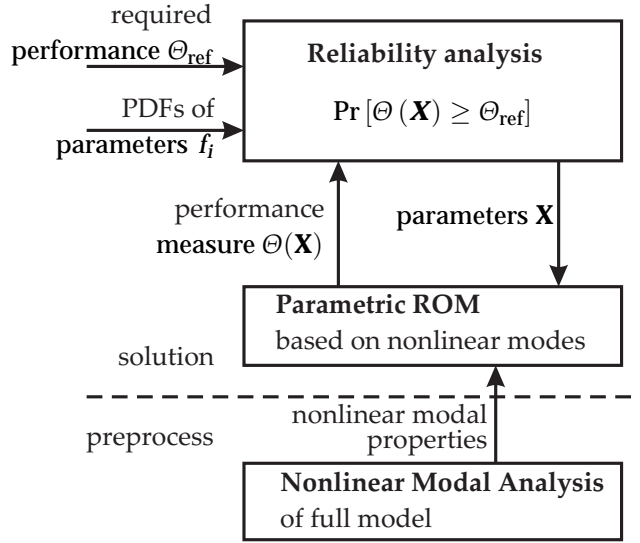


Figure 2: Flow chart of the reliability analysis based on the nonlinear modal ROM

A flow chart of the resulting approach is illustrated in Fig. 2. It consists of two parts, namely the Nonlinear Modal Analysis (NMA as preprocessing part and the solution part that addresses the actual reliability analysis.

The NMA is first carried out as described in Section 4 in order to compute the modal properties, which are required for the ROM creation. These modal properties depend may depend on several system parameters later have to be varied

in course of design optimization. The modal properties have to be computed with respect to only those parameters that are not inherently included in the ROM. For the numerical example in Section 6 this was the case for the friction coefficient.

In the solution step, the constructed ROM can then be utilized for the efficient prediction of the vibration behavior. This prediction has to be allowed for arbitrary points  $\mathbf{X}$  in the parameter space. These points in general do not coincide with the ones for which the modal properties have been computed in the pre-processing step. To this end, a piecewise cubic interpolation between the points available from the NMA was carried out as described in [23].

The reliability can then be computed by numerical integration of the integral in Eq. (7). The integration scheme selects the required sampling points  $\mathbf{X}$  based on the specified integral limits and the performance measures returned by the ROM (black box). The reliability analysis can further be embedded within an optimization procedure in order to actually solve the design problem stated in Eq. (5).

## 6. Numerical example

### 6.1. Problem definition

The proposed reliability optimization strategy was applied to the underplatform damper design of the rotating bladed disk depicted in Fig. 3a. In this proof-of-concept study, several simplifications were made for the model.

- *Cyclic symmetry*: The bladed disk was considered as perfectly tuned. This is a strong restriction of the uncertain parameter domain since this excludes mistuning, i. e. blade-by-blade variations of parameters. Mistuning can in general have an essential effect on energy localization and overall vibration behavior. It should be emphasized that mistuning is mainly relevant for the special application of rotationally periodic structures. Moreover, this simplification facilitates a more detailed analysis of the individual qualitative influences of other parameters.

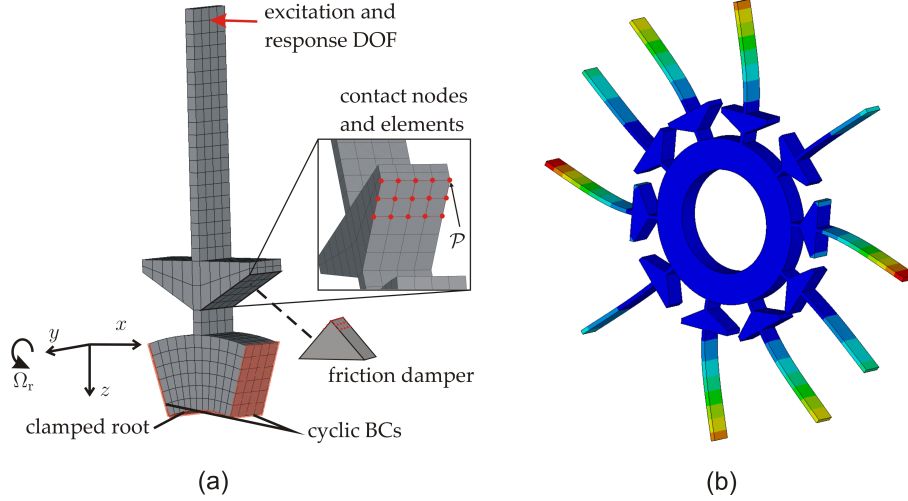


Figure 3: Finite element model of a rotating bladed disk with underplatform dampers ( (a) cyclic segment with boundary conditions, (b) investigated mode shape without friction dampers )

- *Harmonic excitation:* A near-resonant traveling-wave type forcing of engine-order  $EO = 2$  was imposed. The excitation frequency  $\Omega$  is thus directly related to the rotational speed  $\Omega_r$  by  $\Omega = EO\Omega_r$ . It was assumed that the resonant response exhibits the particular symmetry in accordance with the symmetry of excitation and structure [40]. This is not necessarily the case for nonlinear cyclic assemblies [41, 42].
- *Academic geometry:* The geometry in Fig. 3a is a caricature of a realistic geometry of a turbomachinery bladed disk.
- *Simplified damper modeling:* The underplatform wedge dampers were assumed to be rigid, which is a common simplification. The damper mass has a significant influence on the normal preload in the contact interfaces, which in turn has an essential effect on the damping performance. This influence on the normal preload was taken into account in the present case study. In practice, the variation of the damper mass is achieved by variation of damper geometry or material properties. In general these

modifications have an influence on inertial and elastic forces within the assembly, and may affect its dynamic behavior. These influences were found to play a minor role for the relevant mass ranges in the considered parameter studies. This has also been found by other researchers [43, 44]. Hence, only the nominal damper with mass  $m_{\text{opt,c}}$ , as defined later, was considered for the derivation of the structural dynamical properties. During variation of the mass in the following parameter study, only its influence on the normal preload was therefore taken into account.

- *Simplified centrifugal effects:* The normal preload of the contact interfaces was determined from the static equilibrium with the centrifugal force  $mr_{\text{cg}}\Omega_{\text{r}}^2$ , where  $r_{\text{cg}}$  is the distance from the rotation axis to the center of gravity of the dampers. Moreover, the structural matrices of the assembly were regarded as constant within the considered rotational speed range. Hence, centrifugal stiffening was only taken into account for nominal rotor speed of the bladed disk without dampers.
- *Discrete forcing and proportional damping:* In state-of-the-art forced response analyses, the fluid-structure interaction is commonly modeled in terms of external forcing and aerodynamic damping. The external forces are caused by the rotation of the bladed disk in the inhomogeneous (steady) fluid pressure field. Instead of applying an actual fluctuating pressure field, a discrete excitation force at the location indicated in Fig. 3a was specified in this case study. The aerodynamic damping was approximated as weak proportional damping  $\mathbf{C} = i\eta\mathbf{K}$ .
- *Fixed boundary conditions:* The disk was considered to be fixed to a rigid hub without consideration of rotor unbalance or multistage influence. Gyroscopic influences were neglected.

The first two simplifications could only be released by extending the proposed ROM approach to non-harmonic forcing and nonlinear modal interactions. The remaining simplifications are assumed not to have a significant qualitative in-

fluence on the vibration behavior and could be easily taken into account for an actual industrial case study.

Structural and underplatform damper contact dynamics were modeled employing a FE model and 3D contact constraints imposed at discrete contact interfaces, cf. Fig. 3a. This is crucial in order to obtain a complexity of the nonlinear dynamic analysis that is realistic for industrial applications [45, 46, 47]. A homogeneous distribution of the initial normal pressure at the contact interface was assumed. It is conjectured that a more comprehensive modeling of the initial normal pressure distribution would not affect the dynamic analysis complexity, which was the primary motivation for the proposed model reduction approach.

For the design problem, only the first mode of spatial harmonic index 2 was investigated. The deformed mode shape of this mode is illustrated in Fig. 3b. The performance measure was specified as the maximum vibration amplitude,  $a$ , of the response DOF indicated in Fig. 3a. The damper mass  $m$  was considered as the only design variable. Uncertainties in the excitation level  $\varepsilon$ , the linear damping  $\eta$  and the friction coefficient  $\mu$  were taken into account. The design problem can thus be stated as

$$\begin{aligned} & \text{maximize} && \Pr[a(\mathbf{X}) \leq a_{\text{ref}}] \\ & \text{with respect to} && X_{\text{DV}} = m \\ & \text{subject to uncertainties} && \mathbf{X}_{\text{UC}} = [\varepsilon \ \eta \ \mu]^T. \end{aligned} \quad (8)$$

The nominal parameter values  $\mathbf{X}_0 = [m_0 \ \varepsilon_0 \ \eta_0 \ \mu_0]^T$  were specified as  $\mathbf{X}_0 = \begin{bmatrix} m_{\text{opt},c} & 1 & 0.15\% & 0.3 \end{bmatrix}^T$ , where  $m_{\text{opt},c}$  refers to the mass that minimizes the response  $a$  for otherwise nominal parameters.

Arbitrary probability density functions (PDFs)  $f_i$  are allowed in Eq. (7). In practice it is certainly not trivial to determine realistic PDFs  $f_i$  by means of measurements, error estimations and experience. Hence, the parameters that describe the PDFs will often be uncertain themselves. It is thus interesting to vary these parameters and estimate their influence on the robust design [35]. In this study, a gaussian stochastic distribution was assumed for all parameters.



Hence the probability integral in Eq. (7) would have to be evaluated on an infinite domain. In this study, the numerical integration is restricted to the  $3 - \sigma$ -range corresponding to the 99.73rd percentile of the parameter domain. It is important to note that the gaussian distribution is of course also defined for negative parameters, which might lead to questionable results in case of e. g. the friction coefficient. The variabilities investigated in this study, however, lead to negligible probability for negative parameter values in general.

## 6.2. Nonlinear modal properties

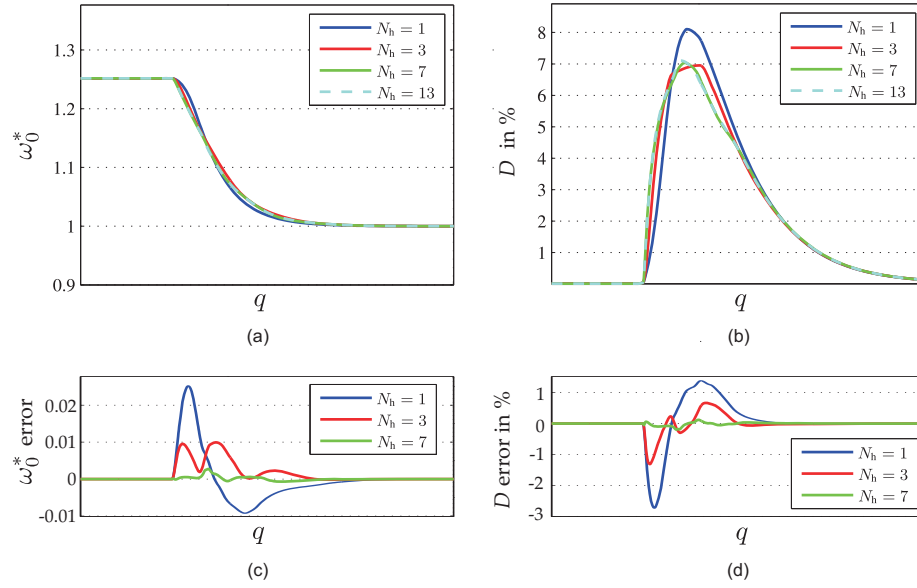


Figure 4: Convergence of modal properties with respect to harmonic order  $N_h$  ( (a) eigenfrequency, (b) modal damping ratio, (c) eigenfrequency error compared to  $N_h = 13$ , (d) modal damping ratio error compared to  $N_h = 13$  )

*Results for nominal parameters.* The nonlinear modal properties for the considered mode have at first been computed for nominal parameters and are illustrated in Fig. 4. Throughout this section, variables indicated by an asterisk (\*) were normalized to the forced resonant case without dampers for nominal

parameters. The modal amplitude  $q$  refers to maximum kinetic energy. The typical friction damping effect can be ascertained from the variation of the modal properties with the modal amplitude: When the entire contact area is stuck, there is no friction damping and the eigenfrequency is constant. For moderate amplitudes, a maximum damping value is reached in the microslip regime and a softening effect can be deduced from the decreasing eigenfrequency. For large amplitudes, the modal damping decreases again and the system asymptotically approaches quasi-linear behavior.

Several harmonics are required to reach asymptotic convergence of the modal properties. A harmonic order  $N_h = 7$  was considered as sufficient regarding the modal analysis results and the small error compared to  $N_h = 13$ , see Figs. 4c-d. Consequently all integer harmonics from the zeroth to the seventh were retained for all further investigations, including the HBM reference computations. In addition to the zeroth and fundamental harmonic, all harmonics up to order were at least locally in the vicinity of the contact interfaces, significant contributions of the higher harmonics are induced by the nonlinear contact forces. This can also be seen from the invariant manifold depicted in Fig. 5 in the coordinates of the contact node  $\mathcal{P}$  (see Fig. 3a). It is generally interesting to investigate the spatial distribution of the contact state. Owing to the simplicity of the geometry and the assumed homogeneous normal pressure distribution, however, the contact dynamics and states were found to be largely homogeneous. Hence, the spatial contact distribution was not illustrated in this paper.

*Influence of the friction coefficient.* In order to conduct the reliability optimization, the nonlinear modes not only have to be available for nominal parameters but for the entire parameter domain spanned by the system parameters  $\mathbf{X} = [m \varepsilon \eta \mu]^T$ . Owing to the assumptions described in Subsection 6.1, the mass  $m$  was varied without re-computation of the modal basis by exploiting the scale invariance as derived in Subsection 2.2. Also, the forcing amplitude  $\varepsilon$  and the weak linear damping  $\eta$  are inherently included in the parameter space of the ROM. Only for the friction coefficient  $\mu$ , the nonlinear modes had to be

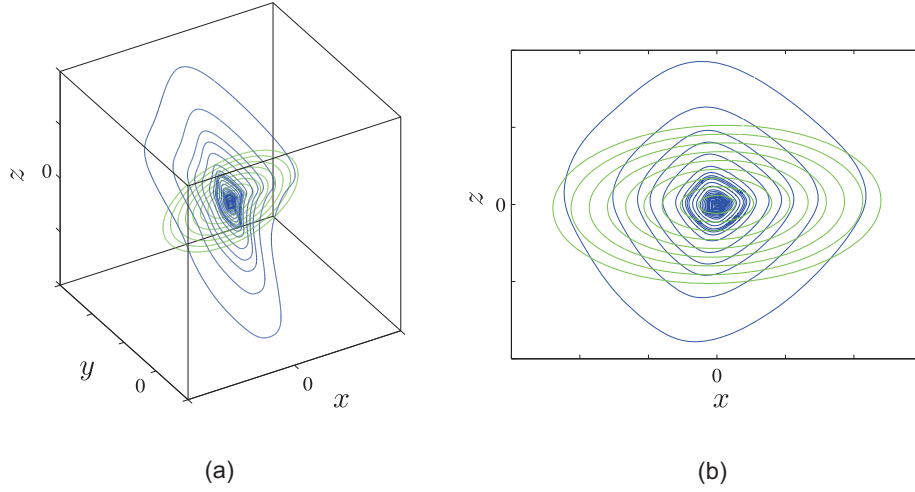


Figure 5: Invariant manifold of nonlinear mode represented as orbits of contact node  $\mathcal{P}$ ; lightly plotted curves corresponds to the linear mode for entirely stuck contact conditions ( (a) three dimensional representation, (b) two dimensional representation )

re-computed.

The modal properties are depicted with respect to the friction coefficient and the modal amplitude in Fig. 6. For a friction contact with constant normal load, the characteristic would only be shifted along the modal amplitude axis. In this case however, the normal dynamics influence the stick-slip transitions. For larger friction coefficients, also larger relative motion amplitudes are required to achieve the same amount of slipping. For larger amplitudes, however, also longer lift-off phases occur during one vibration cycle in case of variable normal loading. Thus, the maximum damping capacity is decreased for larger friction coefficients.

### 6.3. Forced response and sensitivities

In order to assess the accuracy of the ROM compared to direct HBM, the frequency response functions are depicted in Fig. 7 for different damper mass values. For Fig. 7a, the normal preload has been fixed to the value corresponding to the centrifugal force at nominal rotor speed  $\Omega_r^*$ . For Fig. 7b, the influence of the rotor speed  $\Omega_r \neq \Omega_r^*$  on the normal preload was taken into account. Ap-

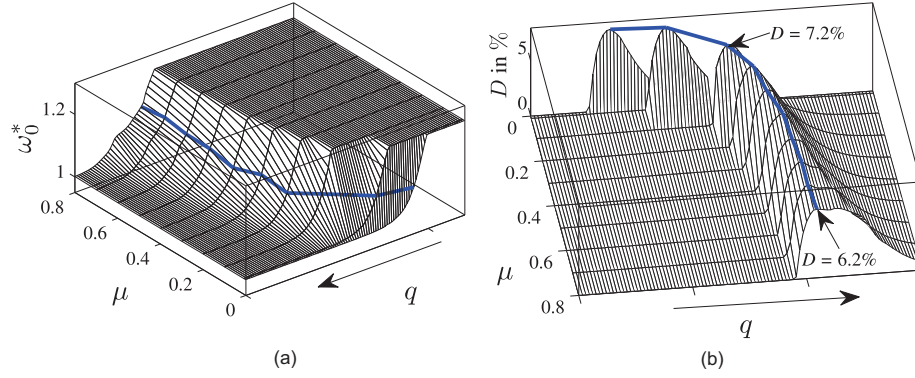


Figure 6: Modal properties as a function of modal amplitude and friction coefficient ( (a) eigenfrequency, (b) modal damping ratio )

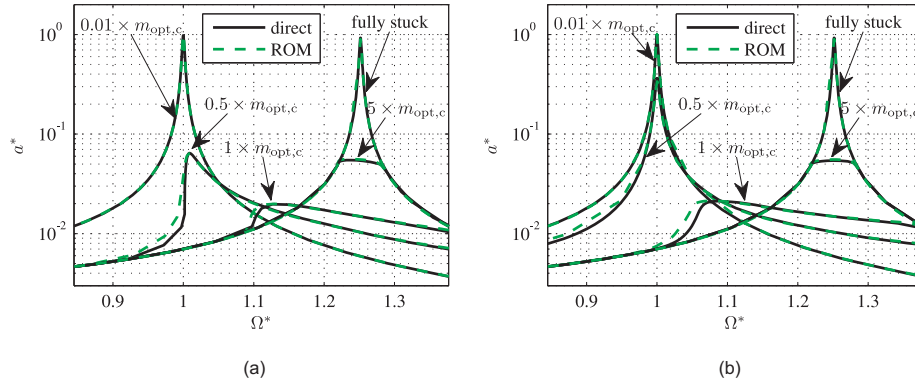


Figure 7: Frequency response functions for different damper mass values ( (a) normal preload treated as fixed, (b) normal preload increasing quadratically with rotational speed )

parently, the effect of the speed-dependent preload is significant in this case. Hence, this effect was considered for the analyses presented in the sequel of this paper. Generally, a very good agreement can be ascertained between direct and ROM computations. This applies in particular to the results in vicinity of resonance which are of primary interest for the reliability. The resonant amplitudes according to the ROM were found to deviate from the direct HBM reference by less than 1% for the results depicted in Fig. 7.

The maximum forced response is depicted in Fig. 8 for varying system parameters. The influence of the mass corresponds to the frequency response results

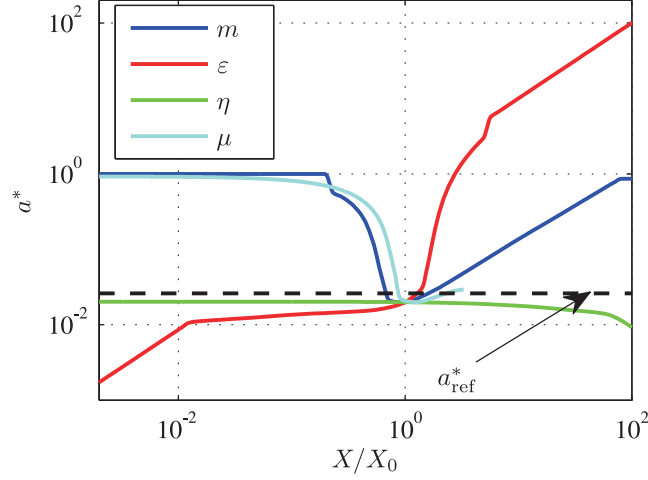


Figure 8: Sensitivity of maximum forced response amplitude with respect to uncertain parameters at  $m = m_0$

illustrated in Fig. 7b. In the field of friction damping, the amplitude-mass characteristic is also known as optimization or bucket curve. The amplitude-excitation level characteristic is also known as damper performance curve [11] and exhibits the often reported flat region where the damper is most effective. The influence of the linear damping factor is small near the nominal value of  $\eta_0 = 0.15\%$  since it is virtually negligible compared to the friction-induced damping of several percents, see Fig. 4b. The effect of the friction coefficient is qualitatively similar to the influence of the damper mass.

#### 6.4. Reliability optimization

*Influence of the reference performance.* The reference performance  $a_{\text{ref}}$  has an essential influence on the reliability characteristic with respect to the design variable  $m$ , see Fig. 9. Only the excitation level was considered as uncertain in this case with a standard deviation of 15%. For very low reference amplitudes, the reliability tends to zero since a certain amount of forced response cannot be avoided. For very large reference amplitudes, the reliability tends to 100% since the vibration amplitudes will be bounded in general. Between these extreme cases, the reliability assumes a bell-like shape. The optimum reliability

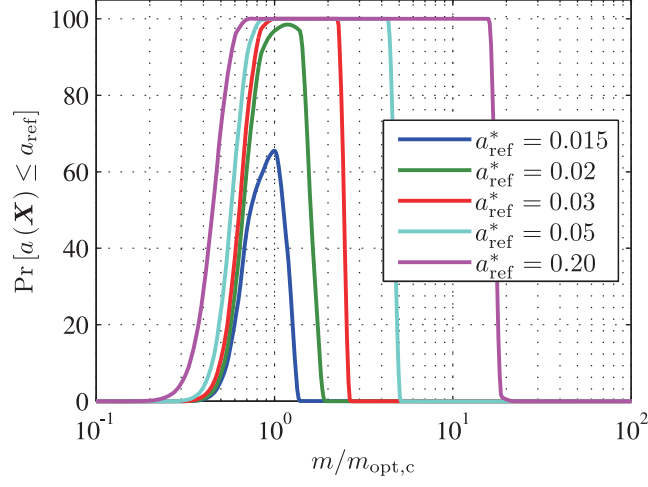


Figure 9: Reliability for different reference amplitude values  $a_{\text{ref}}$

is typically achieved for mass values larger than the mass value that minimizes the vibration amplitudes for nominal parameters. Beyond a certain reference amplitude, specific ranges of mass values perform equally well with a reliability of 100%. It should be noticed that the reference performance is considered as a parameter that is typically a known input parameter for a specific design study. For the following analyses, a value of  $a_{\text{ref}}^* = 0.02$  is chosen, corresponding to a desired vibration reduction by a factor of 50 compared to the case without dampers, cf. Fig. 8.

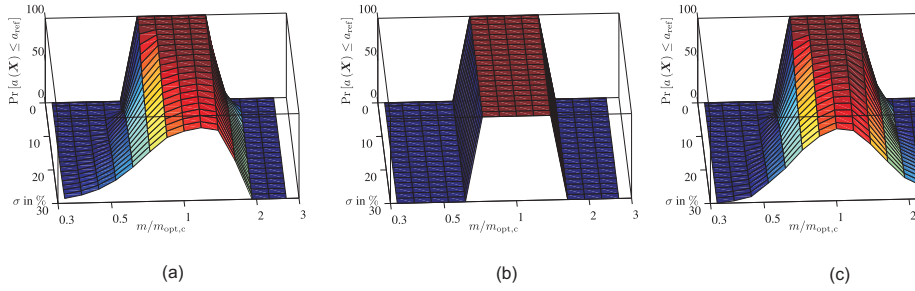


Figure 10: Reliability as a function of the damper mass and the variability of the parameters ( (a) excitation level, (b) linear damping, (c) friction coefficient )

*Influence of parameter variability.* In Fig. 10, the reliability-mass characteristic is illustrated with respect to the variability of the individual parameters. For a standard deviation of zero, the reliability is a step function, i. e. it is either one or zero, depending on whether the reference amplitude is exceeded for nominal parameters. For increasing variability in the parameters the reliability flattens with respect to mass. The location of the optimum mass seems not to be influenced significantly by the variability in the parameters. The reliability characteristic is a step function for uncertainty in  $\eta$ , at least up to a standard deviation of 30%. This is a consequence of the comparatively low sensitivity of the amplitude  $a$  with respect to  $\eta$  as illustrated in Fig. 8.

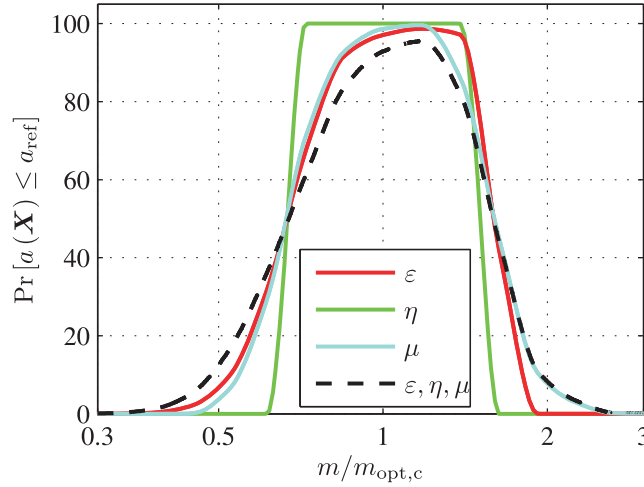


Figure 11: Reliability for different sets of uncertain parameters

*Influence of cumulative uncertainty.* In Fig. 11, the reliability characteristic is illustrated for individual and cumulative uncertainty in the parameters. The standard deviation of all parameters was set to 15%. The cumulation of uncertainties leads to a flatter shape of the resulting reliability characteristic compared to the individual characteristics. The influence is qualitatively similar to the influence of increasing individual variabilities, see Fig. 10.

*Discussion of the optimized damper mass.* As it can be concluded from the previous paragraphs that the optimum robust design depends on different influences such as the reference performance and the parameter variabilities. A significant improvement of the design robustness can only be expected if these properties are specified with care. For the case when all parameters are uncertain with a standard deviation of 15%, the robust damper mass is 17% larger than the optimum damper mass without uncertainties  $m_{\text{opt},c}$ , cf. Fig. 11. Compared to  $m_{\text{opt},c}$ , the robust mass improves the reliability by 2.6% from 93% to 96%, but it reduces the nominal performance by 6.7% in this case. It should be noticed that these values clearly depend on the considered system.

Table 1: Computational effort normalized to overhead caused by single NMA, the asterisk in the last column denotes that the values were estimated based on the single FRF computation times

task	no. of FRF	comp. time	comp. time	comp. time
	evaluations	NMA overhead	ROM	direct (HBM)
single FRF	1	1.0	0.03	1.7
Fig. 9	$9.2 \cdot 10^3$	1.0	276	$1.5 \cdot 10^4$ *
Fig. 11	$2.9 \cdot 10^6$	10.0	$8.9 \cdot 10^4$	$5.0 \cdot 10^6$ *

*Computational cost reduction achieved by the ROM.* In the course of computation, it was generally found that there is a sufficient agreement between ROM and reference calculations. The ROM is therefore qualified for the reliability optimization.

In Tab. 1, the computation times for different tasks are listed. It was found that the average computational effort for computing a single FRF by the direct HBM is in the order of magnitude of a single NMA computation. This is plausible since the mathematical problem dimension is almost the same for each solution point, and a similar number of solution points is required for both analysis types [23]. While the direct HBM computes the FRF branches left and right from the resonance, the NMA determines the resonant amplitude-frequency relationship,



i.e. the backbone curve. In the presented case, the direct HBM computation of a single FRF takes longer than the NMA computation. It is thus already beneficial to follow the ROM approach, despite the NMA overhead.

The benefit of the ROM approach becomes more prominent as soon as multiple FRF calculations are required for different parameter sets.  $9.2 \cdot 10^3$  FRF calculations were required to obtain the results in Fig. 9. Since in this case all varied parameters are readily included in the parameter space of the ROM, the NMA overhead is not increased compared to a single FRF computation. In contrast, the friction coefficient is not included in the inherent ROM parameter space. The NMA was carried out for ten sampling points of the friction coefficient and interpolation was used between these points to obtain the results in Fig. 11. Hence, the NMA overhead was larger in this case. Nevertheless, it can be concluded from Tab. 1 that the NMA overhead is negligible compared to the actual computations required for the probabilistic analysis results presented in Fig. 9 and Fig. 11.

Finally, it has to be remarked that the actual computation times required for the forced response evaluations depend on many influences such as the problem dimension, type of nonlinearity and the considered dynamic regime. The number of function evaluations required for the probabilistic analyses depend on the number of uncertain parameters and the integration method utilized for the evaluation of the expectation integral.

## 7. Conclusions

A novel robust design approach for friction-damped structures was proposed and investigated in terms of a proof-of-concept study. The objective of the design problem is defined as the reliability, i.e. the probability that a specified performance is achieved. For the case study of a bladed disk with friction dampers, the optimum design improved the reliability and insensitivity with respect to uncertain parameters. The robust optimum damper mass was found to be larger than its counterpart for nominal parameters. It is common prac-

tice to design the damper mass larger than its theoretical optimum value. The proposed objective gives rise to a probabilistic justification for this practice and provides means for a quantitative approaches towards robust design of friction interfaces for the purpose of vibration damping.

The probabilistic nature of the numerical approach results in a severely increased computational burden compared to the analysis of the deterministic model. The proposed approach was found to become prohibitive in conjunction with models of realistic complexity. Hence, a drastic ROM approach based on the concept of nonlinear modes was introduced to the probabilistic design approach. A recently developed multi-harmonic multi-modal ROM was therefore extended regarding the parameter space required for design approach. The computational effort was reduced by several orders of magnitude.

Several opportunities for future work arise from the findings of this paper. It would be desirable to alleviate the simplifications made for the numerical example and investigate a more realistic case study. Regarding bladed disks, it would be interesting to investigate the influence of blade-by-blade varying parameters.

## **Appendix A. Proof of scale invariance for systems with piecewise linear contact constraints**

In [23], the scale invariance was postulated in the form of a hypothesis. The validity was demonstrated by numerical examples only and no strict mathematical proof was provided. The proof is derived for the initial value problem in time domain in order to show its broad range of validity. For convenience, the ODE in Eq. (1) is written in state space notation,

$$\dot{\mathbf{y}}(t) + \begin{bmatrix} -\dot{\mathbf{u}}(t) \\ \mathbf{M}^{-1} (\mathbf{K}\mathbf{u}(t) + \mathbf{C}\dot{\mathbf{u}}(t) + \mathbf{g}(\mathbf{u}(t), \dot{\mathbf{u}}(t), \Delta) - \mathbf{f}_e(t)) \end{bmatrix} = \mathbf{0},$$

$$\mathbf{y}(t=0) = \mathbf{y}_0. \quad (\text{A.1})$$

Herein, the state vector is  $\mathbf{y}^T = [\mathbf{u}^T \ \dot{\mathbf{u}}^T]$ . The parameter  $\Delta$  can also be a linear function in the components of displacement  $\mathbf{u}$  or velocity  $\dot{\mathbf{u}}$ . For this parameter, the scale invariance in Eq. (4) is derived in the following.

Note that the validity of Eq. (4) is obvious in the linear case with  $\mathbf{g} \equiv 0$ . In the nonlinear case, the validity of Eq. (4) boils down to the requirement

$$\mathbf{g}(\kappa \mathbf{u}(t), \kappa \dot{\mathbf{u}}(t), \kappa \Delta) = \kappa \mathbf{g}(\mathbf{u}(t), \dot{\mathbf{u}}(t), \Delta) . \quad (\text{A.2})$$

The validity of Eq. (A.2) can now be shown element-wise for the vector of non-linear forces  $\mathbf{g}$ . In this study, the proof is restricted to the unilateral spring nonlinearity and the elastic Coulomb nonlinearity defined in Eq. (3), since these are the only nonlinearities involved in the contact constraint formulations employed in this study.

For the unilateral spring nonlinearity, the parameter  $\Delta$  is the preload  $p_0$ . The requirement in Eq. (A.2) can be easily verified by substitution:

$$p_n(\kappa u_n, \kappa p_0) = (k_n \kappa u_n + \kappa p_0)_+ = \kappa (k_n u_n + p_0)_+ = \kappa p_n(u_n, p_0) . \quad (\text{A.3})$$

For each contact node, the tangential friction dynamics depend on the normal dynamics. Since the normal contact law is scalable, also the limiting friction force  $\mu p_n$  is scalable. Thus, for convenience,  $\Delta = \mu p_n$  can be defined as scaling parameter for the friction law. With this, the requirement in Eq. (A.2) can be proven for the friction law:

$$\begin{aligned} \mathbf{p}_t(\kappa \mathbf{u}_t, \kappa \Delta^*) &= \begin{cases} \mathbf{0} & \text{lift-off} \\ k_t(\kappa \mathbf{u}_t - \kappa \mathbf{u}_t(t_{\text{stick}})) + \kappa \mathbf{p}_t(t_{\text{stick}}) & \text{stick} \\ \kappa \Delta^* \frac{\kappa \dot{\mathbf{u}}_t}{\|\kappa \dot{\mathbf{u}}_t\|} & \text{slip} \end{cases} \\ &= \kappa \begin{cases} \mathbf{0} & \text{lift-off} \\ k_t(\mathbf{u}_t - \mathbf{u}_t(t_{\text{stick}})) + \mathbf{p}_t(t_{\text{stick}}) & \text{stick} \\ \Delta^* \frac{\dot{\mathbf{u}}_t}{\|\dot{\mathbf{u}}_t\|} & \text{slip} \end{cases} \\ &= \kappa \mathbf{p}_t(\mathbf{u}_t, \Delta^*) . \end{aligned} \quad (\text{A.4})$$

The proof needs to be completed by demonstrating the scalability of the transition conditions:

transition conditions:

$$\begin{aligned} \text{stick-slip transition:} \quad & \|\kappa \mathbf{p}_t\| = \kappa \Delta^* \Leftrightarrow \|\mathbf{p}_t\| = \Delta^*, \\ \text{slip-stick transition:} \quad & \|k_t \kappa \dot{\mathbf{u}}_t\| = \kappa \dot{\Delta}^* \Leftrightarrow \|k_t \dot{\mathbf{u}}_t\| = \dot{\Delta}^*. \end{aligned} \quad (\text{A.5})$$

Note that the validity of the scale invariance in time domain such as in Eq. (1) implies the validity in frequency domain such as in the NMA. Hence, the scale invariance can be exploited to obtain the solution of nonlinear eigenproblem for a parameter value  $\kappa \Delta$  from the computed solution for  $\Delta$ . Thus, the treatment of the normal preload as an inherent parameter of the ROM, as proposed in Section 4 is an exact approach in terms of the contact constraints used in this study.

## References

- [1] M. Berthillier, C. Dupont, R. Mondal, J. J. Barrau, Blades Forced Response Analysis with Friction Dampers, *Journal of Vibration and Acoustics* 120 (2) (1998) 468–474.
- [2] L. Panning, W. Sextro, K. Popp, Spatial Dynamics of Tuned and Mistuned Bladed Disks with Cylindrical and Wedge-Shaped Friction Dampers, *International Journal of Rotating Machinery* 9 (3) (2003) 219–228.
- [3] E. P. Petrov, D. J. Ewins, Effects of Damping and Varying Contact Area at Blade-Disk Joints in Forced Response Analysis of Bladed Disk Assemblies, *Journal of Turbomachinery* 128 (2) (2006) 403–410.
- [4] D. Charleux, C. Gibert, F. Thouverez, J. Dupeux, Numerical and Experimental Study of Friction Damping in Blade Attachments of Rotating Bladed Disks, *International Journal of Rotating Machinery* (2006) 1–13.

- [5] S. Tatzko, L. Panning-von Scheidt, J. Wallaschek, A. Kayser, G. Walz, Investigation of Alternate Mistuned Turbine Blades Non-Linear Coupled by Underplatform Dampers, Paper GT2013-95681, Proceedings of ASME Turbo Expo 2013, June 3-7, San Antonio, TX, USA (2013).
- [6] D. N. Mavris, Bandte O., Delaurentis D. A., Robust design simulation: A probabilistic approach to multidisciplinary design, *Journal of Aircraft* 36 (1) (1999) 298–307.
- [7] B. D. Yang, C. H. Menq, Modeling of Friction Contact and Its Application to the Design of Shroud Contact, *Journal of Engineering for Gas Turbines and Power* 119 (4) (1997) 958–963.
- [8] L. Panning, W. Sextro, K. Popp, Optimization of Interblade Friction Damper Design, Paper 2000-GT-0541, Proc. of ASME Turbo Expo 2000, Power for Land, Sea and Air, May 8-11, Munich, Germany (2000).
- [9] D. Laxalde, F. Thouverez, J. P. Lombard, Vibration Control for Integrally Bladed Disks Using Friction Ring Dampers, Paper GT2007-27087, Proc. of GT2007, ASME Turbo Expo 2007: Power for Land, Sea and Air, May 14-17, Montreal, Canada (2007).
- [10] L. Huyse, Padula S. L., Lewis R. M., Li W., Probabilistic approach to free-form airfoil shape optimization under uncertainty, *AIAA Journal* 40 (9) (2002) 1764–1772.
- [11] T. M. Cameron, J. H. Griffin, R. E. Kielb, T. M. Hoosac, An Integrated Approach for Friction Damper Design, *Journal of Vibration and Acoustics* 112 (2) (1990) 175–182.
- [12] D. Cha, D. Sinha, Computation of the Optimal Normal Load of a Friction Damper Under Different Types of Excitation, *Journal of Engineering for Gas Turbines and Power* 125 (4) (2003) 1042–1049.
- [13] E. P. Petrov, A sensitivity-based method for direct stochastic analysis of nonlinear forced response for bladed discs with friction interfaces, Paper

- GT2007-27981, Proc. of GT2007, ASME Turbo Expo 2007: Power for Land, Sea and Air, May 14-17, Montreal, Canada (2007).
- [14] E. P. Petrov, Analysis of sensitivity and robustness of forced response for nonlinear dynamic structures, *Mechanical Systems and Signal Processing* 23 (1) (2009) 68–86.
  - [15] P. Kumar, S. Narayanan, Response statistics and reliability analysis of a mistuned and frictionally damped bladed disk assembly subjected to white noise excitation, in: *Proceedings of the ASME Turbo Expo*, Vol. 6, 2010, pp. 649–658.
  - [16] R. R. Craig, Coupling of substructures for dynamic analysis: An overview, Paper AIAA-2000-1573 (2000).
  - [17] C. Pierre, A. A. Ferri, E. H. Dowell, Multi-Harmonic Analysis of Dry Friction Damped Systems Using an Incremental Harmonic Balance Method, *Journal of Applied Mechanics* 52 (4) (1985) 958–964.
  - [18] E. P. Petrov, Direct Parametric Analysis of Resonance Regimes for Nonlinear Vibrations of Bladed Discs, Paper GT2006-90147, Proc. of GT2006, ASME Turbo Expo 2006: Power for Land, Sea and Air, May 8-11, Barcelona, Spain (2006).
  - [19] A. Vakakis, L. Manevitch, Y. Mikhlin, V. Pilipchuk, A. Zevin, *Normal modes and localization in nonlinear systems*, John Wiley & Sons, 2008.
  - [20] G. Kerschen, M. Peeters, J. C. Golinval, A. F. Vakakis, Nonlinear normal modes, Part I: A useful framework for the structural dynamicist: Special Issue: Non-linear Structural Dynamics, *Mechanical Systems and Signal Processing* 23 (1) (2009) 170–194.
  - [21] C. Touzé, M. Amabili, Nonlinear normal modes for damped geometrically nonlinear systems: Application to reduced-order modelling of harmonically forced structures, *Journal of Sound and Vibration* 298 (4–5) (2006) 958–981.

- [22] F. Blanc, C. Touzé, J.-F. Mercier, K. Ege, A.-S. Bonnet Ben-Dhia, On the numerical computation of nonlinear normal modes for reduced-order modelling of conservative vibratory systems, *Mechanical Systems and Signal Processing* 36 (2) (2013) 520–539.
- [23] M. Krack, L. Panning-von Scheidt, J. Wallaschek, A method for nonlinear modal analysis and synthesis: Application to harmonically forced and self-excited mechanical systems, *Journal of Sound and Vibration* 332 (25) (2013) 6798–6814.
- [24] M. Krack, L. Panning-von Scheidt, J. Wallaschek, A. Hartung, C. Siewert, Reduced Order Modeling Based on Complex Nonlinear Modal Analysis and its Application to Bladed Disks With Shroud Contact, Paper GT2013-94560, *Proceedings of ASME Turbo Expo 2013*, June 3-7, San Antonio, TX, USA (2013).
- [25] K. L. Johnson, *Contact mechanics*, repr. Edition, Cambridge University Press, Cambridge, 1989.
- [26] C. Siewert, L. Panning, A. Schmidt-Fellner, A. Kayser, The estimation of the contact stiffness for directly and indirectly coupled turbine blading, Paper GT2006-90473, *Proc. of ASME Turbo Expo*, ASME Turbo Expo 2006: Power for Land, Sea and Air, May 08-11, Barcelona, Spain (2006).
- [27] E. P. Petrov, D. J. Ewins, Analytical Formulation of Friction Interface Elements for Analysis of Nonlinear Multi-Harmonic Vibrations of Bladed Disks, *Journal of Turbomachinery* 125 (2) (2003) 364–371.
- [28] C. M. Firrone, S. Zucca, M. M. Gola, The effect of underplatform dampers on the forced response of bladed disks by a coupled static/dynamic harmonic balance method, *International Journal of Non-Linear Mechanics* 46 (2) (2011) 363–375.
- [29] M. Krack, L. Panning-von Scheidt, J. Wallaschek, A High-Order Harmonic

Balance Method for Systems With Distinct States, *Journal of Sound and Vibration* 332 (21) (2013) 5476–5488.

- [30] P. Wriggers, *Computational contact mechanics*, Springer, 2006.
- [31] W. Sextro, *Dynamical Contact Problems with Friction: Models, Methods, Experiments and Applications*, Ph.D. thesis, University of Hannover, Hannover (2002).
- [32] L. Panning, W. Sextro, K. Popp, Optimization of the Contact Geometry between Turbine Blades and Underplatform Dampers with Respect to Friction Damping, Paper 2002-GT-30429, *Proc. of ASME TURBO EXPO 2002*, June 3-6, Amsterdam, Netherlands (2002).
- [33] J. Szwedowicz, W. Sextro, R. Visser, P. A. Masserey, On Forced Vibration of Shrouded Turbine Blades, Paper GT-2003-38808, *Proc. of ASME Turbo Expo 2003*, Power for Land, Sea, and Air, June 16-19, Atlanta, Georgia, USA (2003).
- [34] S. Nacivet, C. Pierre, F. Thouverez, L. Jezequel, A Dynamic Lagrangian Frequency-Time Method for the Vibration of Dry-Friction-Damped Systems, *Journal of Sound and Vibration* 265 (1) (2003) 201–219.
- [35] M. Krack, L. Panning-von Scheidt, J. Wallaschek, C. Siewert, A. Hartung, Robust Design of Friction Interfaces of Bladed Disks With Respect to Parameter Uncertainties, Paper GT2012-68578, *Proc. of ASME Turbo Expo 2012*, June 11-15, Copenhagen, Denmark (2012).
- [36] M. Krack, L. Panning-von Scheidt, C. Siewert, A. Hartung, J. Wallaschek, Analysis and Robust Design of Friction Joints for Vibration Reduction in Bladed Disks, Paper-ID 224, *Proc. of SIRM 2013 – 10th International Conference on Vibrations in Rotating Machines*, February 25-27, Berlin, Germany (2013).
- [37] P. J. Davis, P. Rabinowitz, *Numerical integration*, Blaisdell Publishing Company London, 1967.



- [38] M. Pfaffrath, U. Wever, Stochastic Integration Methods: Comparison and Application to Reliability Analysis, Paper GT2012-68973, Proc. of ASME Turbo Expo 2012, June 11-15, 2012, Copenhagen, Denmark (2012).
- [39] D. Laxalde, L. Salles, L. Blanc, F. Thouverez, Non-Linear Modal Analysis for Bladed Disks with Friction Contact Interfaces, Paper GT2008-50860, Proc. of GT2008, ASME Turbo Expo 2008: Power for Land, Sea and Air, June 9-13, Berlin, Germany (2008).
- [40] C. Siewert, M. Krack, L. Panning, J. Wallaschek, The Nonlinear Analysis of the Multiharmonic Forced Response of Coupled Turbine Blading, Paper ISROMAC12-2008-20219, Proc. of The 12-th International Symposium on Transport Phenomena and Dynamics of Rotating Machinery, Honolulu, Hawaii, March 17-22 (2008).
- [41] M. E. King, A. F. Vakakis, A Very Complicated Structure of Resonances in a Nonlinear System with Cyclic Symmetry: Nonlinear Forced Localization, *Nonlinear Dynamics* 7 (1) (1995) 85–104.
- [42] F. Georgiades, M. Peeters, G. Kerschen, J. C. Golinval, M. Ruzzene, Non-linear Modal Analysis and Energy Localization in a Bladed Disk Assembly, Paper GT2008-51388, Proc. of ASME Turbo Expo 2008: Power for Land, Sea and Air, GT2008, June 9-13, Berlin, Germany, pp. 1-8 (2008).
- [43] K. Y. Sanliturk, D. J. Ewins, A. B. Stanbridge, Underplatform Dampers for Turbine Blades: Theoretical Modeling, Analysis, and Comparison With Experimental Data, *Journal of Engineering for Gas Turbines and Power* 123 (4) (2001) 919–929.
- [44] M. H. Jareland, A Parametric Study of a Cottage Roof Damper and Comparison with Experimental Results, Paper 2001-GT-0275, Proc. of ASME TURBO EXPO 2001, June 4-7, New Orleans, Louisiana, USA (2001).
- [45] M. Krack, A. Herzog, L. Panning-von Scheidt, J. Wallaschek, C. Siewert, A. Hartung, Multiharmonic Analysis and Design of Shroud Friction

Joints of Bladed Disks Subject to Microslip, Paper DETC2012-70184, Proc. of ASME 2012 International Design Engineering Technical Conferences & Computers and Information in Engineering Conference (IDETC/CIE 2012), August 12-15, Chicago, USA (2012).

- [46] C. Siewert, L. Panning, J. Wallaschek, C. Richter, Multiharmonic Forced Response Analysis of a Turbine Blading Coupled by Nonlinear Contact Forces, *Journal of Engineering for Gas Turbines and Power* 132 (8) (2010) 082501–082509.
- [47] S. Zucca, C. M. Firrone, M. Gola, Modeling underplatform dampers for turbine blades: a refined approach in the frequency domain, *Journal of Vibration and Control* 19 (7) (2013) 1087–1102.